Finite-Difference Kirchhoff Migration

Carlos Cunha[1], Gerson Ritter[1], Fernanda Thedy[1], Alexandre Sardinha[1] and Nelson Hargreaves[1] ([1]Petrobras)

This paper was prepared for presentation during the 16th International Congress of the Brazilian Geophysical Society held in Rio de Janeiro, Brazil, 19-22 August 2019.

Abstract

A new imaging method, blending some features of the Reverse Time Migration with the Kirchhoff algorithm is presented in this article.

The Common-Offset Kirchhoff migration computes an output image point from the convolution of every input trace with compact source-to-image and image-to-receiver Green functions. In practice, these compact Green functions are represented by travel-time and amplitude tables.

While in Kirchhoff time migration the Green functions are analytically computed using a simplified representation of the propagation medium, in depth migration it is necessary to use more computationally complex methods, such as ray tracing or numerical solutions to the Eikonal equation. In general, in these methods only the first arrival is computed and represented in the travel time tables, which is not always the most important contribution to the image in a complex medium.

A method is proposed in this paper in which the Green functions are computed with the propagation of the wave equation using a finite-difference algorithm identical to the one used in Reverse Time Migration and compacted to represent only the most energetic events.

Introduction

All the imaging methods used in the industry are based on solutions of the wave equation. They usually differ in the approximation used in their implementation. The 3D Common-Offset Kirchhoff Migration, for example, in its more general expression can be defined as the following integral:

$$I(\vec{x},\vec{h}) = \iiint FG(\vec{\xi} - \vec{h}, z_S, \vec{x}, t') \frac{\partial D(\vec{\xi},\vec{h},t)}{\partial t} G(\vec{\xi} + \vec{h}, z_R, \vec{x}, t - t')\, dt'\, dt\, d\vec{\xi}$$

Eq. 1

where: $\vec{x}$ is the image coordinate (x, y, z); $\vec{h}$ is the half-offset vector (h_x, h_y); $\vec{\xi}$ is the surface position vector (x_m, y_m) of the mid-point of each trace of the common-offset volume defined by $|\vec{h}|$; $\eta = \eta(\vec{\xi} + \vec{h})$ e $\epsilon = \epsilon(\vec{\xi} - \vec{h})$ are the source and receiver depth of each trace, respectively; $G(\vec{x_1}, \vec{x_2}, t')$ represents the Green Function between two points; D is the common-offset input data to be migrated associated to $|\vec{h}|$; and F is defined such as $I(\vec{x}, \vec{h})$ is an approximation of the subsurface reflectivity. In this representation the Green functions associated to a point $\vec{x}$ of the migrated volume are three-dimensional wavefields.

The Green function $\mathbf{G}(\overrightarrow{\mathbf{x_1}}, \overrightarrow{\mathbf{x_2}}, \boldsymbol{t'})$ in its simplest form can be represented by just the amplitude and traveltime of a single event between the points $\overrightarrow{\mathbf{x_1}}$ and $\overrightarrow{\mathbf{x_2}}$, that is, $\mathbf{G}(\overrightarrow{\mathbf{x_1}}, \overrightarrow{\mathbf{x_2}}, \boldsymbol{t'}) = \mathbf{A}(\overrightarrow{\mathbf{x_1}}, \overrightarrow{\mathbf{x_2}})\boldsymbol{\delta}[\boldsymbol{t'} - \boldsymbol{\tau}(\overrightarrow{\mathbf{x_1}}, \overrightarrow{\mathbf{x_2}})]$, where $\boldsymbol{\tau}(\overrightarrow{\mathbf{x_1}}, \overrightarrow{\mathbf{x_2}})$ is the traveltime table between point $\overrightarrow{\mathbf{x_1}}$ where source or receivers are located and subsurface point $\mathbf{x_1}$.

The computation of the Green function is usually done by a specialized module that computes its value for all the positions of image volume and it is stored in travel-time tables. These times can be computed by, for example, ray-tracing, or solving the eikonal equation. In this paper it is computed by a finite-difference algorithm.

Wave propagation by finite-difference

The wavefield P resulting from a source S is described, at any point in space and at any instant in time, by the wave equation, which in its acoustic version reads:

$$\frac{\partial^2 \boldsymbol{P}}{\partial \boldsymbol{t}^2} - \boldsymbol{v}^2 \boldsymbol{\nabla}^2 \boldsymbol{P} = \boldsymbol{\delta}(\boldsymbol{x_S})\boldsymbol{\delta}(\boldsymbol{y_S})\boldsymbol{\delta}(\boldsymbol{z_S})\boldsymbol{S}(\boldsymbol{t})$$

The equation describes the propagation of an acoustic wave in its entire complexity, which includes primary reflections, multiple reflections, direct arrivals, refractions, multiple arrivals, among other phenomena. Not only is the travel time described, but also the wave amplitude.

The wave propagation can also be computed in an elastic or visco-elastic medium. The most important impact in the use of these different wave equations in the method will be in its computational cost.

The finite-difference method solves the wave equation using a discrete propagation grid, where the wavefield P is evaluated in the whole volume in successive steps of time. This algorithm is the basis of the Reverse Time Migration. In this paper this solution is used to compute the Green functions expressed as travel times and amplitude tables used by Kirchhoff migration.

There are two main difficulties in using finite-difference propagation to compute travel time tables: the computational cost and the complexity of wavefield.

The cost is proportional to the fourth power of the maximum propagation frequency. If a low enough frequency is used the cost can be acceptable. Note that the travel time is weakly dependent on the maximum frequency of the source wavelet, although the size of the grid imposes some limits on the resolution of the travel time. For the prospects where this method were tested, a maximum frequency of 21 Hz gave the best balance between time and cost of propagation and the migration results. In some cases, the maximum frequency may vary according to the complexity of the medium.

Regarding the complexity of the wavefield is necessary to define what events are to be measured. The travel time table, used in Kirchhoff migration, stores, for a given source point, only one time value for each subsurface position. In a finite-difference wave propagation it is possible to have more than one time associated to a given point. For example, the downgoing first arrival and later an upgoing reflection. Or two different downgoing arrivals in different times, which is usually called multiple arrivals.

Compact Green functions

Figure 1 exemplifies the process of representing travel times as compact Green functions. (a) shows a snapshot at the time 0.8 s of a wavefield, or the Green function, associated to a point source in the Marmousi velocity model. Overlaid to it there is the isochronous curve associated to the most energetic event. Note that not always the maximum energy corresponds to the first arrival. For each point in the isochronous there is an amplitude value that is also stored in a corresponding amplitude table. (b) shows the most energetic part of the Green function at various snapshots taken 0.16 s apart. And in (c) the isochronous at same times as in (b), but computed solving the eikonal equation. It is observed the increased difference between the most energetic arrivals computed by finite-difference and the first arrivals computed by the eikonal.

Although in this example only the most energetic arrival is measured to build the travel time tables, it is possible to get the second, third or more most energetic arrivals and keep the corresponding travel times and amplitudes in separate tables. These could be used to implement a multi-arrival Kirchhoff migration, for example.

The amplitude information naturally measured together with the travel time can also be used as input to the Kirchhoff algorithm, providing better image amplitude when compared to other methods.

Wavefield separation

High angle reflection events sometimes show with their amplitudes anomalously large. Although in rare cases they can contribute to the imaging of events weakly illuminated by the direct wave, they are mostly responsible by the formation of false events.

It was thus chosen to use only direct arrivals, even when reflected information has larger amplitude. To accomplish this, the wavefield is separated in down-going energy, associated with the direct wave, and up-going energy, generally associated with reflections. Partial tables associated with each field are computed, and they are merged using the smallest time associated with each point. In this case, the direct is preserved even when it belongs to upgoing turning waves.

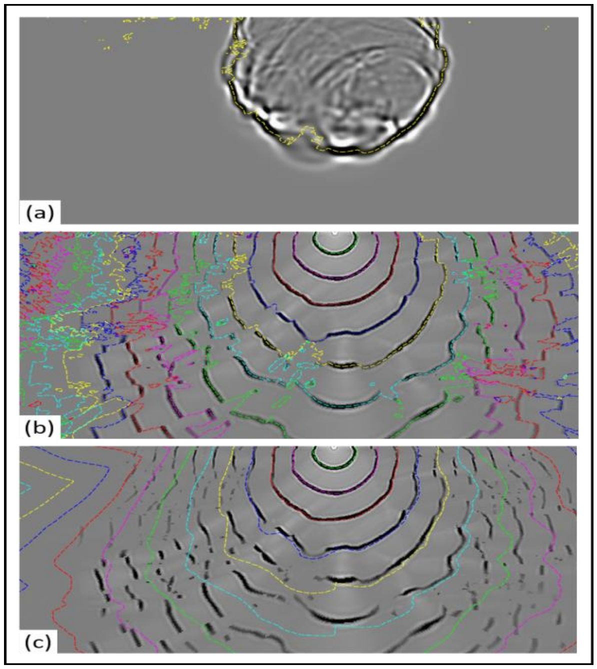

Figure 1: (a) Time-slice for t=0.8s of the complete wavefield with the most energetic arrival overlaid. (b) Compacted Green Function sampled at every 0.16 s with only the most energetic events shown. (c) Same compacted Green Function as in (b), but the eikonal isochronous curves overlaid.

Finite difference Kirchhoff migration in Marmousi

The 2D Marmousi synthetic dataset was used to test and validate the finite-difference Kirchhoff Migration. It is well known that conventional first arrival Kirchhoff imaging does not produce a clear image of the Marmousi “reservoir”.

In the test, two travel time tables were computed with the finite-difference algorithm, with the first and second most energetic arrivals, respectively. For reference, a travel time table was computed solving the eikonal equation. The data was Kirchhoff migrated with the first arrival eikonal tables, with the most energetic tables and with the two most energetic tables. Additionally, a RTM image was created as a benchmark.

The results are presented in Figure 2. It is observed that the image obtained with finite-difference computed tables are clearly superior to that using the eikonal table, especially in the fault system and the region below it. The quality of both finite-difference Kirchhoff is similar to the RTM, but with better frequency content. It also shows small difference between the one and two arrivals images.

The computational cost of the Kirchhoff migration, represented by equation 1, increases as a function of the square of the number of events if all combinations of source and receiver Green functions are taken into account. In practice, the contribution of weaker events can be discarded. The cost of creating multiple tables for many events is low compared to the propagation, but the additional memory required can be an issue.

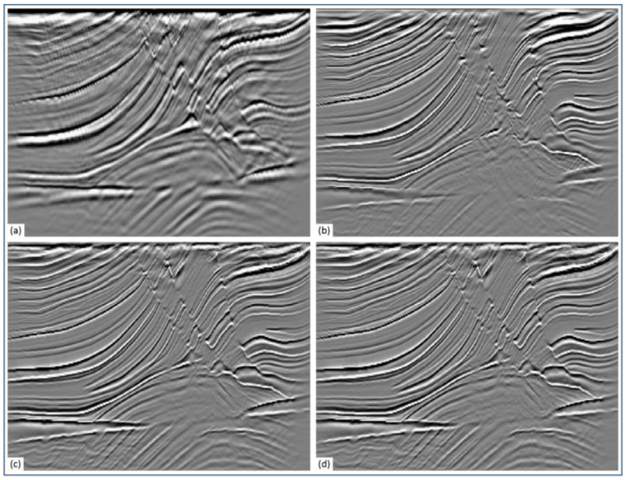

Figure 2: Marmousi test (a) RTM image.(b) Kirchhoff with eikonal travel time; (c) Kirchhof with finite-difference, first strongest event; (d) Kirchhof with finite-difference, first and second strongest events

Real data results

Seismic 3D data in a Santos basin area was selected to test the method in a more real life environment.

Figure 3 shows two Kirchhoff migrated common image gathers using finite-difference and eikonal travel time tables. It is observed that the top of salt presents a good quality reflection at longer offsets in the finite-difference CIG than in the eikonal one. This can be attributed to the faster arrival of the top of salt refraction event mapped in the eikonal method. In the finite-difference method the most energetic is the top of salt reflection which is the correctly imaged.

Figures 4 and 5 show the corresponding migrated stacks from finite-difference and eikonal Kirchhoff

Conclusions

The finite-difference Kirchhoff presented here has the following advantages over the conventional first arrival Kirchhoff or RTM imaging algorithms:

- It is better than conventional Kirchhoff in handling wavefield propagation in complex subsurface velocity models. It can even use multi arrivals.
- It is easier and cheaper to generate common image gather than RTM;
- It is much cheaper than RTM;
- Unlike RTM, the cost of imaging (as all Kirchhoff-based methods) does not depend on the desired frequency bandwidth

The finite-difference Kirchhoff migration was able to image the top of salt at longer offsets compared to a first arrival method. This could potentially be useful to better estimate the propagation velocity, and especially the epsilon anisotropy parameter.

Acknowledgments

The geophysicists Luiz Alberto Santos and André Romanelli Rosa made important contributions that led to the development of the method presented.

We would like to thank Petrobras for permission to publish this paper.

References

Rosa, A. L. R., 2010, Análise do Sinal Sísmico, editado pela Sociedade Brasileira de Geofísica.

Andrade, P. N., Pestana, E. C., and Santos, A. W. G., 2015, Kirchhoff Depth Migration using Maximum Amplitude Traveltimes Computed by the Chebychev Polynomial Recursion: Fourteenth International Congress of the Brazilian Geophysical Society

Ehinger, A., Lailly, P., and Marfurt, K. J., 1996, Green's Function Implementation of Common-offset Wave-Equation Migration: Geophysics, 61, 1813-1821.

Etgen, J., 2012, 3D Wave Equation Kirchhoff Migration: SEG Annual Meeting.

Schuster, G. T., 2002, Reverse-Time Migration = Generalized Diffraction Stack Migration: SEG Annual Meeting.

Zhan, G., and Schuster, G. T., 2010, Skeletonized Least Squares Wave Equation Migration: SEG Annual Meeting.

Zhou, M., and Schuster, G. T., 2001, Wave-Equation Wavefront Migration: SEG Annual Meeting.

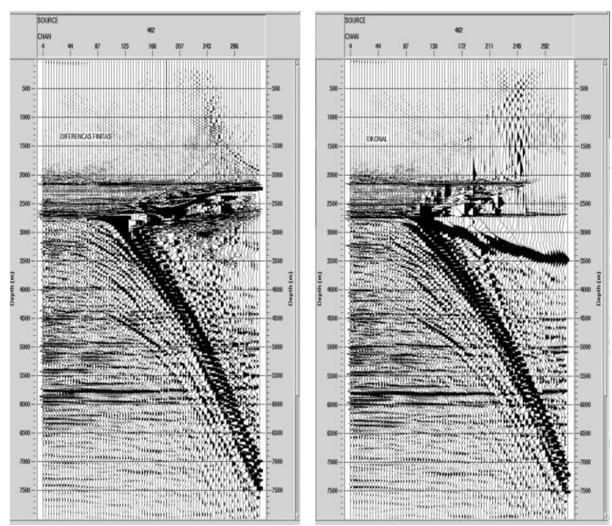

Figure 3: Kirchhoff 3D Common image gathers, migrated with tables from finite-difference method (left) and eikonal (right) .

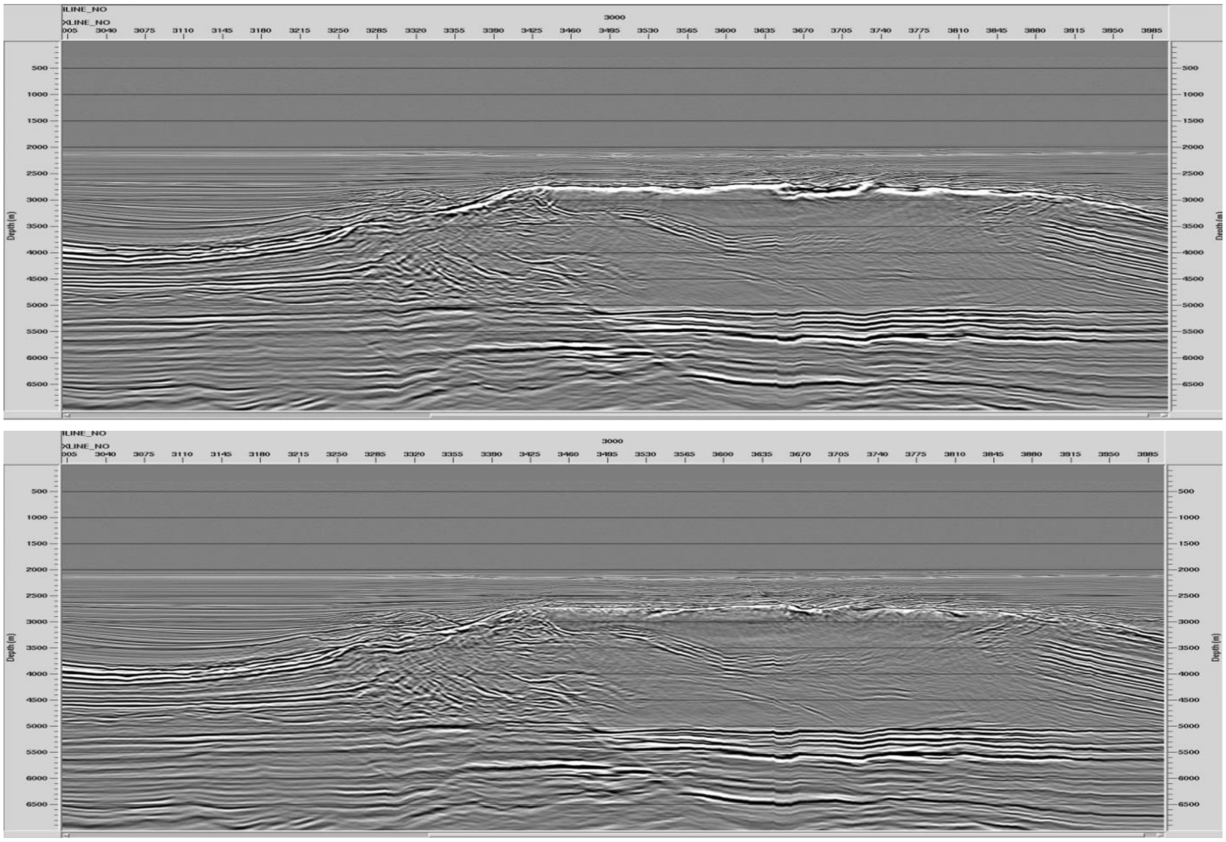

Figure 4: Kirchhoff 3D Common Stack, migrated with tables from finite-difference method (above) and eikonal (below) .

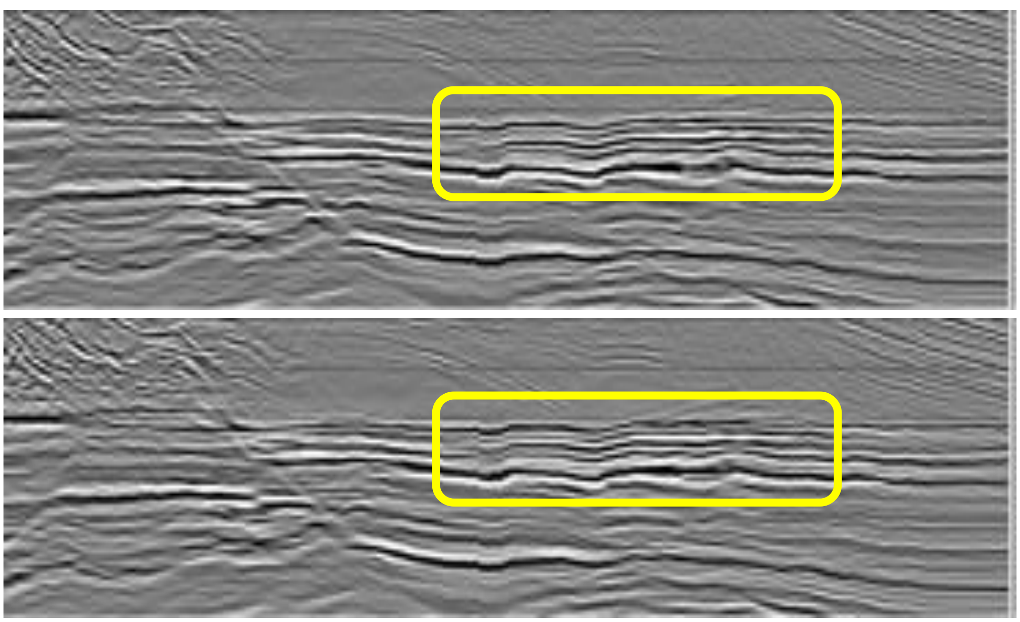

Figure 5: Detail of Figure 4 at the pre salt layers.